

**A Study of the Phase Equilibria in the Cr-Mo-Ni System**

**Karin Frisk**

**TRITA-MAC-0429**

**Mar. 1990**

# A Study of the Phase Equilibria in the Cr-Mo-Ni System

Karin Frisk  
Division of Physical Metallurgy  
Royal Institute of Technology  
Stockholm, Sweden

## Abstract

A thermodynamic evaluation of the Cr-Mo-Ni system has been performed using a computerized optimization procedure. Parameters describing the Gibbs energy of the various phases have been calculated. The intermetallic phases  $\delta$ , P and  $\sigma$  were included in the calculations, using a three-sublattice model. Any phase equilibria can be recalculated from the set of parameters that has been determined, and calculated isothermal sections are compared with experimental data from different sources. A few measurements were made at 1373K in the present work, to supplement previous experimental results. The experimental data used for the optimization, i.e. data at 1523K and 1373K, are well described by the present calculations, but also calculations at other temperatures are in many cases in good agreement with the experimental data.

## 1. Introduction

The objective of the present work was to obtain a thermodynamic description of the Cr-Mo-Ni system. For this purpose available experimental information on the system was studied. A review of the Cr-Mo-Ni system was recently presented by Jena et al.<sup>1</sup> The phase diagram has been investigated experimentally several times, but the results from different studies are in disagreement at low temperatures. In addition to the data reviewed by Jena et al. a recent investigation of the system by Selleby<sup>2</sup> was used in the present analysis. Selleby used a diffusion couple technique, and measured tielines between the various phases using a scanning electron microscope with an energy dispersive X-ray analysis equipment. Three ternary intermetallic phases have been found in this system, the  $\sigma$ , P and  $\mu$  phases, and the  $\delta$  phase from the binary Mo-Ni system extends into the ternary system. These intermediate phases lie very close in composition, and it is difficult to distinguish them from each other only by measuring the composition. The work by Selleby<sup>2</sup> was therefore supplemented in the present work by identifying the phases in some ternary alloys equilibrated at 1373K, by X-ray diffraction. The available experimental data were analysed using thermodynamic models, describing the Gibbs energy of the individual phases. The models involve adjustable parameters that were calculated using a computerized optimization procedure. A set of parameters giving the best fit to the selected experimental data is given and a number of calculated isothermal sections are presented and compared with experimental data.

## 2. Available Experimental Data

### 2.1 Previous Work

The present work is based upon previous evaluations of the binary systems. The Cr-Mo phase diagram<sup>3</sup> is shown in Fig.1, the Cr-Ni phase diagram<sup>4</sup> is shown in Fig.2, and the Mo-Ni<sup>5</sup> phase diagram is shown in Fig.3. In addition to the intermediate phases present in the Mo-Ni system, three ternary intermetallic phases have been found in the Cr-Mo-Ni system, the P,  $\sigma$  and  $\mu$  phases. The P phase was first discovered by Rideout et al<sup>6</sup>, and its composition range has later been measured<sup>7,8</sup>. The composition of the  $\sigma$  phase in equilibrium with the fcc phase and the bcc phase has been measured several times<sup>6-11</sup>. Raghavan et al.<sup>8</sup> studied the phase equilibria in the Ni rich corner of the Cr-Mo-Ni system at 1523 and 1123K. The composition of the phases was measured by X-ray microanalysis, and the structure of the phases was determined by convergent beam diffraction. At 1123K they found that the  $\mu$  phase is stable. This phase has not been reported at higher temperatures, or by other authors at low temperatures, and we do not know up to what temperature it is stable. We therefore decided to leave out the  $\mu$  phase from the present study. Jena et al<sup>1</sup> recently reviewed available experimental data on the equilibria in the Cr-Mo-Ni system. They found that the experimental data from different studies are in reasonably good agreement at 1473 and 1523K, but that there is considerable disagreement at low temperatures.

Two recent studies of the Cr-Mo-Ni system, not included in the review by Jena et al.<sup>1</sup> were considered in the present work. Kodentzov et al.<sup>11</sup> determined the compositions of the P and  $\sigma$  phases in equilibrium with the bcc and fcc phases at 1425K. Selleby measured a number of tielines in the system at 1473, 1373 and 1273K, using a diffusion couple technique. The best data from this study are at 1373K. In the present work a few supplementary measurements were made on ternary alloys equilibrated at 1373K, described below, in good agreement with the data by Selleby<sup>2</sup>.

## 2.2 The Present Work

Four ternary alloys with the mean compositions listed in Table I were prepared by arc melting of compacts obtained from powders. The alloys were sealed in silica capsules under vacuum, and heat treated at 1373K for approximately 350 hours. The samples were quenched in brine, and cut in two parts. One part was used for microcopic examination and the other was crushed for X-ray diffraction examination. The samples were examined in a scanning electron microscope equipped with an energy dispersive X-ray spectrometer (EDS) and LINK AN100000 X-ray microanalysis system. The compositions of the phases present in each sample were measured. In samples No 1 and 4 (see Table I) two phases were present, in sample No 2 three phases were present and sample No 3 was single phase. The measured compositions are shown in Fig.8, together with previous experimental results, in good agreement. The sample No 3 gave the compositions of the three-phase triangle fcc+ $\sigma$ +P, but the phases were not identified. The alloys No 1 and 4 consisted mainly of an intermetallic phase that was identified as the P phase. The phase present in alloy No 3 was identified as the  $\sigma$  phase.

## 3. Selection of experimental data

### 3.1 Solid phases

A set of experimental data was selected from the available data, to be used for the thermodynamic evaluation. Since discrepancies between different authors have been reported at low temperatures, data at high temperatures were first considered. We chose to rely upon data by Raghavan et al.<sup>8</sup> and Bloom and Grant<sup>7</sup> at 1523K, since they are in reasonably good agreement. The examination by Bloom and Grant is also the only investigation that covers an entire composition triangle. Bloom and Grant determined the phase compositions of a large number of alloys, whereas Raghavan et al.<sup>8</sup> measured tielines, and three-phase equilibria. Since tieline information is more useful for the evaluation of thermodynamic parameters, we selected the data by Raghavan et al.<sup>8</sup> for the cases when the two studies are in disagreement. The data by Selleby<sup>2</sup> at 1373K and data from the present work at the same temperature were selected. The examination by Selleby<sup>2</sup> covers a large part of the isothermal section, and the measurements from the present work have confirmed these results. It is very difficult to judge the reliability of the various results from other studies. It was therefore decided to rely only on the data from 1523 and 1373K in a first calculation, and to compare the calculated results with the experimental data from other temperatures, to check the consistency.

### 3.2 The liquidus surface

The data on the liquidus were reviewed by Jena et al.<sup>1</sup>, and based on their conclusions we chose to use the data by Bloom and Grant for the present evaluation. Bloom and Grant<sup>7</sup> measured the liquidus temperatures of a large number of ternary alloys. The minimum temperature found in their work was 1448K, and the maximum temperature was the melting point of Mo. They also presented a schematic system of invariant planes compatible with the experimental results. In the present work the reported liquidus temperatures were used to evaluate the properties of the ternary Cr-Mo-Ni liquid phase.

## 4. Thermodynamic Models

#### 4.1 The bcc, fcc and liquid phases

The bcc, fcc and liquid phases were described by the following substitutional solution model

$$G_m = x_{Cr} \circ G_{Cr} + x_{Mo} \circ G_{Mo} + x_{Ni} \circ G_{Ni} + RT(x_{Cr} \ln x_{Cr} + x_{Mo} \ln x_{Mo} + x_{Ni} \ln x_{Ni}) + {}^E G_m + G_m^{mg} \quad (1)$$

The  $\circ G$  parameters represent the Gibbs energy of the elements in a hypothetical nonmagnetic state, and are taken from previous assessments of Cr<sup>12</sup>, Mo<sup>13</sup> and Ni<sup>14</sup>. All  $\circ G$  values are referred to the enthalpy of the stable state at 298.15K and 0.1MPa, denoted by the superscript SER.  ${}^E G_m$  represents the excess Gibbs energy and is given by

$${}^E G_m = x_{Cr} x_{Mo} L_{Cr,Mo} + x_{Cr} x_{Ni} L_{Cr,Ni} + x_{Mo} x_{Ni} L_{Mo,Ni} + x_{Cr} x_{Mo} x_{Ni} L_{Cr,Mo,Ni} \quad (2)$$

The parameters denoted L represent interactions between the elements. They can be composition dependent according to

$$L_{A,B} = \sum_{i=0}^1 {}^i L_{A,B} (x_A - x_B)^i \quad (3)$$

All L parameters representing interactions between two elements are taken from previous assessments of the Cr-Mo<sup>3</sup>, Cr-Ni<sup>4</sup> and Mo-Ni<sup>5</sup> systems.

$G_m^{mg}$  represents the contribution to magnetic ordering and is described with the functions given by Hillert and Jarl<sup>15</sup>, see Table III.

#### 4.2 The Intermetallic Phases

In the binary Mo-Ni system there are three intermediate phases present, the  $\beta$ ,  $\gamma$  and  $\delta$  phases. At the temperatures studied in the present work only the  $\delta$  phase is stable. It has been modeled<sup>5</sup> with a three-sublattice model<sup>16,17</sup>, based on the crystal structure of the phase. We know that there is a small solubility of Cr in the  $\delta$  phase, and Cr was therefore placed on the first two sublattices, see Table II. The P,  $\mu$  and  $\sigma$  phases exist as ternary compounds in the Cr-Mo-Ni system, and they are not stable in any of the binary systems. These phases have been studied in other systems and we want to make the present work consistent with such recent evaluations, so that they can be combined to calculate equilibria in higher order systems. Therefore the same models were used as in the previous evaluations. For the P phase this means that the same model as for the P phase in the Fe-Mo-Ni system<sup>18</sup> was used. This is a three sublattice model based on measurements of the distribution of different atoms on different sites, and information on the composition range of the P phase, described in more detail in ref.18. Based on the compilation of experimental data concerning the P phase by Sinha<sup>19</sup> we placed Cr on the first two sublattices, as seen in Table II. For the  $\sigma$  phase the binary Cr-Mo and Cr-Ni models have been determined in previous assessments<sup>20,21</sup>, and the model for the ternary  $\sigma$  phase is a combination of these binary models, see Table II.

The  $\delta$  and P phases are described with a model of the type  $(Cr,Ni)_a (Cr,Mo,Ni)_b (Mo)_c$  where a, b and c are the number of sites on each sublattice. From one formula unit of this type the sublattice model<sup>16,17</sup> yields an expression of the Gibbs energy for each phase as follows

$$G_m = {}^1 y_{Cr} ({}^2 y_{Cr} \circ G_{Cr:Cr:Mo} + {}^2 y_{Mo} \circ G_{Cr:Mo:Mo} + {}^2 y_{Ni} \circ G_{Cr:Ni:Mo}) + {}^1 y_{Ni} ({}^2 y_{Cr} \circ G_{Ni:Cr:Mo} + {}^2 y_{Mo} \circ G_{Ni:Mo:Mo} + {}^2 y_{Ni} \circ G_{Ni:Ni:Mo})$$

$$+ aRT ({}^1y_{Cr} \ln {}^1y_{Cr} + {}^1y_{Ni} \ln {}^1y_{Ni}) + bRT ({}^2y_{Cr} \ln {}^2y_{Cr} + {}^2y_{Mo} \ln {}^2y_{Mo} + {}^2y_{Ni} \ln {}^2y_{Ni}) + {}^E G_m \quad (4)$$

${}^i y_M$  denotes the fraction of M (where M is Cr, Ni or Mo) on the sublattice i (i is the sublattice 1 or 2, where there is mixing of atoms).  ${}^\circ G_{Cr:Ni:Mo}$ , as an example, represents the Gibbs energy of the phase in question with Cr on the first sublattice, Ni on the second sublattice and Mo on the third sublattice, and similarly for the other  ${}^\circ G$  parameters. The  ${}^\circ G$  parameters were referred to the selected standard states of the pure elements.

The  $\sigma$  phase is described with the following model  $(Ni)_8(Cr,Mo)_4(Cr,Mo,Ni)_{18}$  and the Gibbs energy expression according to the sublattice model<sup>16, 17</sup> is then

$$\begin{aligned} G_m = & {}^2y_{Cr} ({}^3y_{Cr} {}^\circ G_{Ni:Cr:Cr} + {}^3y_{Mo} {}^\circ G_{Ni:Cr:Mo} + {}^3y_{Ni} {}^\circ G_{Ni:Cr:Ni}) + \\ & {}^2y_{Mo} ({}^3y_{Cr} {}^\circ G_{Ni:Mo:Cr} + {}^3y_{Mo} {}^\circ G_{Ni:Mo:Mo} + {}^3y_{Ni} {}^\circ G_{Ni:Mo:Ni}) \\ & + 4RT ({}^2y_{Cr} \ln {}^2y_{Cr} + {}^2y_{Ni} \ln {}^2y_{Ni}) + 18RT ({}^3y_{Cr} \ln {}^3y_{Cr} + {}^3y_{Mo} \ln {}^3y_{Mo} + {}^3y_{Ni} \ln {}^3y_{Ni}) + {}^E G_m \quad (5) \end{aligned}$$

with all definitions the same as above. In this case i is the sublattice 2 or 3. The excess Gibbs energy ( ${}^E G_m$ ) was in the present work for simplicity set to zero for all phases.

As explained above some of the  ${}^\circ G$  parameters are given from previous evaluations of binary and ternary systems<sup>5, 18, 20, 21</sup>. Since the available information for the evaluation of the remaining  ${}^\circ G$  parameters is very limited, a simplification was introduced. Andersson et al.<sup>22</sup> suggested that the  ${}^\circ G$  parameters can be estimated by comparing the elements on the different sublattices with the values for the elements in the bcc or fcc state. An element on a sublattice with a coordination number of 12 is compared with the fcc state of the element and an element on sublattices with coordination number of 14 or higher are compared with the bcc state of the element. Using this suggestion, the elements on the first sublattice, that correspond to elements on sites with coordination number (CN) of 12, are compared with fcc. Elements on the two second sublattices (CN14, CN15 or CN16) are compared with the bcc state. For our example above, we thus get

$${}^\circ G_{Cr:Ni:Mo} = a {}^\circ G_{Cr}^{fcc} + b {}^\circ G_{Ni}^{bcc} + c {}^\circ G_{Mo}^{bcc} + \Delta {}^\circ G_{Cr:Ni:Mo} \quad (6)$$

and similarly for all other  ${}^\circ G$  parameters, see Table III. The term  $\Delta {}^\circ G_{Cr:Ni:Mo}$  is a correction term that is evaluated from experimental data.

## 5. Parameter Evaluation

The evaluation of the thermodynamic parameters was made by means of a computer optimization program developed by Jansson<sup>23</sup>. The thermodynamic parameters were determined to give the best agreement between calculated phase equilibria and the selected set of experimental data. The optimization was performed in steps. The data on the fcc/fcc+ $\sigma$  phase boundary at 1523K by Raghavan et al.<sup>8</sup> were in the first step used to evaluate the  $\sigma$  phase parameters. It was assumed that there are no ternary interactions in the bcc and the fcc phases. Two ternary parameters and the binary Mo-Ni parameters for the  $\sigma$  phase were evaluated from these data, and all interaction parameters were set to zero. Thereafter, the P and  $\delta$  phases were fitted into the diagram, by determining the binary parameters for the Cr-Mo side of the diagram, and the ternary parameters for P and  $\delta$ . A reasonably good description of the Ni rich side of the diagram was obtained. From the data by Bloom and Grant<sup>7</sup>, we know the approximate compositions of the intermetallic phases in

equilibrium with the bcc phase. In addition, measured tielines for these equilibria are available at 1373K, from the study by Selleby<sup>2</sup>, and from the present work. The data from 1373K were therefore used in a second step of the optimization, together with the data at 1523K. The position of the fcc+P+ $\sigma$  three-phase triangle is known at both temperatures, and the bcc+ $\delta$ +P and the fcc+ $\delta$ +P equilibria have been measured at 1373K<sup>2</sup>. The position of the bcc+P+ $\sigma$  three phase triangle is approximately known from the data by Selleby at 1373K. The temperature dependence of the P phase parameters could thus be determined. The data at 1473K were compared with calculated values during the optimization. The results obtained from the optimization using the data at 1523K and 1373K showed reasonable agreement with the data by Class et al.<sup>9</sup> and by Selleby<sup>2</sup> at 1473K, and was therefore accepted. All evaluated parameters are summarized in Table III.

## 6. Discussion of Results

The calculated isothermal section of the Cr-Mo-Ni system at 1523K is shown in Fig.4. In Fig.5 the same calculated section is compared with experimental data from Raghavan et al.<sup>8</sup> at 1523K. The three-phase triangles are reasonably well reproduced by the calculation, and the compositions of the various phases are reproduced within the limit of experimental uncertainty. In Fig.6 the calculated section at 1523K is compared with the experimental data by Bloom and Grant<sup>7</sup>. This diagram shows that the data by Bloom and Grant<sup>7</sup> disagree with Raghavan et al.<sup>8</sup> on the position of the fcc+ $\sigma$ +P three-phase equilibria, and in the present work we trusted the latter. Further, there is quite a large difference on the position of the measured fcc phase boundary between the two studies. However, the calculation describes quite well the data by Bloom and Grant on the bcc+ $\sigma$  and the bcc+fcc+ $\sigma$  equilibria, that were not measured by Raghavan et al.. As explained above, the optimization was made using the data from 1373K as well as the data from 1523K. The calculated isothermal section at 1373K is shown in Fig.7. In Fig.8 the calculated section is compared with experimental data by Selleby<sup>2</sup>, and from the present work. The tielines measured in the present work are marked with symbols. All the other tielines were measured by Selleby. The three-phase triangle, fcc+ $\sigma$ +P, measured in the present work is quite well reproduced by the present calculation. The fcc+ $\delta$ +P and bcc+ $\delta$ +P three phase triangles, both measured by Selleby<sup>2</sup>, are well described by the calculation. The experiments indicate that the  $\sigma$  phase in equilibrium with the bcc phase should have a lower Ni content. This could not be described with the model used for the  $\sigma$  phase, since the minimum Ni content allowed by the model is 27 at%. As explained above, the model for  $\sigma$  was already fixed in previous evaluations. The remaining phase boundaries lie within the range of experimental error (2-3%), and the description was not further refined.

With the thermodynamic parameters fixed to fit the data at 1523K and 1373K, isothermal sections at other temperatures were calculated and compared with experimental data. The calculated isothermal section at 1473K is shown in Fig.9. It is compared with the data by Class et al.<sup>9</sup> and with the three-phase triangles given by Rideout et al.<sup>6</sup> in Fig.10. The agreement is acceptable. The measured fcc/fcc+ $\sigma$  phase boundary could not be reproduced with the description of the Cr-Ni system used in the present work. In Fig.11 the calculated isothermal section at 1425K is compared with experimental data by Morizot and Vignes<sup>10</sup> and Kodentzov et al.<sup>11</sup>. These data indicate that the  $\sigma$  phase should have a larger existence range, both in equilibrium with the fcc phase and with the bcc phase. On the fcc phase boundary the agreement between the two experimental studies is poor, and the calculation shows that the data by Kodentzov et al.<sup>11</sup> are in best agreement with data at other temperatures. Jena et al.<sup>1</sup> pointed out some experimental sources of error in the experimental work of Morizot and Vignes<sup>10</sup>, and no comparison with their data from lower temperatures was therefore made. The calculated isothermal section at 1273K is shown in

Fig.12. In Fig.13 the calculation is compared with experimental data by Selleby<sup>2</sup>. There are some inconsistencies in the experimental results, but the agreement with the calculation is reasonable. In Fig.14 the calculation at 1273K is compared with the data by Class et al.<sup>9</sup>. The positions of the intermetallic phases are in quite good agreement, but the measured fcc phase is again in disagreement with the binary Cr-Ni system. The calculated section at 1123K, excluding the  $\mu$ ,  $\beta$  and  $\gamma$  phases is shown in Fig.15. In Fig.16 this calculation is compared with the experimental data by Raghavan et al.<sup>8</sup> concerning the P and  $\sigma$  phases. The agreement is reasonable, except for the composition of the P phase. The experimental data indicated that the  $\mu$  phase should be interposed between the  $\delta$  and the P phases at this temperature.

### The liquid phase

The calculated projection of the liquidus surface with all ternary interactions set to zero is shown in Fig.17. The dashed lines are isotherms. The isotherms are compared with the experimental data by Bloom and Grant<sup>7</sup> in Fig.18. Since the agreement is good, no ternary parameters were evaluated.

## 7. Summary

The thermodynamic parameters presented in the present work were evaluated from experimental data at 1523K and 1373K. The calculations concerning the solid phases presented above show that the present description of the Cr-Mo-Ni system reproduces most of the experimental data between 1273K and 1523K well. The major discrepancies are on the fcc/fcc+intermetallic phase boundaries, where the experimental data from different studies are in disagreement. However, the agreement of the calculated fcc phase boundary with the data by Raghavan et al.<sup>8</sup>, by Selleby<sup>2</sup> and with the present work is acceptable. The present calculation also agrees reasonably well with the data on the fcc+ $\sigma$  phase boundary measured by Raghavan et al.<sup>8</sup> at 1123K. The experimental liquidus surface is well described by the calculations without adding any ternary interaction parameters for the liquid phase. A complete description of the thermodynamic properties of the Cr-Mo-Ni system has thus been obtained, that in many cases compares well with experimental data.

## Acknowledgements

I wish to thank Prof.M.Hillert for useful advice, constructive criticism and for the help received during the preparation of this paper. I also wish to thank Nils Lange for the help with the experimental work. The alloys used in this study were supplied by Sandvik AB. All diagrams were calculated using the Thermo-Calc databank developed by Drs. Bo Sundman, Bo Jansson and Jan-Olof Andersson at the Division of Physical Metallurgy<sup>24</sup>.

## References

1. A.K.Jena, S.B.Rajendraprasad and K.P.Gupta, *J. Alloy Phase Diagrams*, 1989, Vol. 5, pp. 164-177.
2. M.Selleby, Bachelor Thesis, Division of Physical Metallurgy, Royal Institute of Technology, Stockholm, Sweden.
3. K.Frisk and P.Gustafson, *CALPHAD*, 1988, Vol. 12, pp. 247-254.
4. T.Chart, NPL, Tedington, UK, unpublished work.
5. K.Frisk, *CALPHAD*, 1990, vol. 14(4), pp. 371-80.

6. S.Rideout, W.D.Manly, E.L.Kamen, B.S.Lement and P.A.Beck, Trans. AIME, 1951, Vol. 191, pp. 872-876.
7. D.S.Bloom and N.J.Grant, J. Metals, 1954, Vol. 6, pp. 261-268.
8. M.Raghavan, R.R.Mueller, G.A.Vaughn and S.Floreen, Met. Trans. A, 1984, Vol. 15A, pp. 783-792.
9. I.Class, H.Gräfen and E.Scheil, Z. Metallkunde, 1962, Vol. 53, pp. 283-293.
10. C.Morizot and A.Vignes, Mem. Sci. Rev. Metallurgique, 1973, Vol. 70, pp. 857-874.
11. A.A.Kodentsov and S.F.Dunaev and E.M.Slusarenko, J. Less Comm. Met., 1988, Vol. 141, pp. 225-234.
12. J-O.Andersson, Int. J. Thermophysics, 1985, Vol. 6, pp. 411-419.
13. A.Fernández Guillermet, Int. J. Thermophysics, 1985, Vol. 6, pp. 367-393.
14. A.T.Dinsdale, "SGTE data for pure elements", Report DMA(A)195, National Physics Laboratory, 1989.
15. M.Hillert and M.Jarl, Calphad 2 (1978) 227-238.
16. M.Hillert and L-I.Staffansson, Acta. Chem. Scand., 1970, vol. 24, pp. 3618-26.
17. B.Sundman and J.Ågren, J.Phys. Chem. Solids, 1981, vol. 42, pp. 297-301.
18. K.Frisk, Trita-Mac-0428, Div. Phys. Met, Royal Inst. Techn., Stockholm, Sweden, 1990.
19. A.K.Sinha, Progress in Materials Science, 1972, vol.15., pp.115-118.
20. P.Gustafsson, Trita-Mac-0320, Div. Phys. Met, Royal Inst. Techn., Stockholm, Sweden, 1986.
21. J-O. Andersson and N.Lange, Met. Trans. A, 1988, vol. 19A, pp. 1385-1394.
22. J-O.Andersson, A.Fernández Guillermet, M.Hillert, B.Jansson and B.Sundman, Acta Metall., 1986, vol. 34, pp. 437-445.
23. B.Jansson, PhD Thesis, The Royal Institute of Technology, Stockholm, Sweden, 1984.
24. B.Sundman, B.Jansson and J-O.Andersson, Calphad 9 (1985) 153.

**Table I** Composition of the ternary alloys used in the present study, and specifications on the heat treatments.

Notation	Composition (atomic %)	Heat Treatment	
		Temperature	Time(hours)
Alloy 1	55%Cr 15%Mo 30%Ni	1373K	354
Alloy 2	30%Cr 30%Mo 40%Ni	1373K	354
Alloy 3	20%Cr 45%Mo 35%Ni	1373K	354
Alloy 4	10%Cr 59%Mo 31%Ni	1373K	331

**Table II** Models for the Intermetallic Phases

Phase	Model	Reference to previous assessment
$\delta$	$(Cr,Ni)_{24}(Cr,Mo,Ni)_{20}(Mo)_{12}$	5,18
P	$(Cr,Ni)_{24}(Cr,Mo,Ni)_{20}(Mo)_{12}$	18
$\sigma$	$(Ni)_8(Cr,Mo)_4(Cr,Mo,Ni)_{18}$	18,20,21

**Table III** Summary of the thermodynamic parameters describing the Cr-Mo-Ni system. All values are given in SI units. The parameters evaluated in the present work are noted with an asterisk (\*). The descriptions of the binary systems are taken from refs.3-5. The parameters for the P and  $\sigma$  phases that were not evaluated in the present work, are taken from refs.18 and 20. The values are valid for one formula unit of the phases.

The magnetic contribution to Gibbs energy is described by:  $G_m^{mg} = RT \ln(\beta+1)f(\tau)$ ,  $\tau=T/T_c$

$$\text{for } \tau < 1 : f(\tau) = 1 - \left[ \frac{79\tau^{-1}}{140p} + \frac{474}{497p} \left( \frac{\tau^3}{6} + \frac{\tau^9}{135} + \frac{\tau^{15}}{600} \right) \right] / A$$

$$\text{and for } \tau > 1 : f(\tau) = - \left( \frac{\tau^{-5}}{10} + \frac{\tau^{-15}}{315} + \frac{\tau^{-25}}{1500} \right) / A$$

$$\text{where } A = \left( \frac{518}{1125} \right) + \left( \frac{11692}{15975} \right) \left[ \frac{1}{p} \left( \frac{\tau}{\tau-1} \right) - 1 \right] \text{ and } p \text{ depends on the structure.}$$

### The Liquid Phase

1 sublattice, Constituents Cr,Mo,Ni

$$298.15 < T < 2180.00 : {}^\circ G_{Cr}^{Liquid} = {}^\circ G_{Cr}^{bcc} + 24335.93 - 11.42 T + 2.37615 \cdot 10^{-21} T^7$$

$$2180.00 < T < 6000.00 : {}^\circ G_{Cr}^{Liquid} = {}^\circ G_{Cr}^{bcc} + 18405 - 8.562 T + 2.88526 \cdot 10^{32} T^{-9}$$

$$298.15 < T < 2896.00 : {}^\circ G_{Mo}^{Liquid} = {}^\circ G_{Mo}^{bcc} + 41616.757 - 14.6085 T + 4.03583 \cdot 10^{-22} T^7$$

$$2896.00 < T < 5000.00 : {}^\circ G_{Mo}^{Liquid} = {}^\circ G_{Mo}^{bcc} + 34262.098 - 11.9419 T + 4.610447 \cdot 10^{33} T^{-9}$$

$$298.15 < T < 1728.00 : {}^\circ G_{Ni}^{Liquid} = {}^\circ G_{Ni}^{fcc} + 16414.686 - 9.397 T - 3.82318 \cdot 10^{-21} T^7$$

$$1728.00 < T < 3000.00 : {}^\circ G_{Ni}^{Liquid} = {}^\circ G_{Ni}^{fcc} + 18290.88 - 10.537 T - 1.12754 \cdot 10^{31} T^{-9}$$

$$L_{Cr,Mo}^{Liquid} = +15810 - 6.714 T - 6220(x_{Cr} - x_{Mo})$$

$$L_{Cr,Ni}^{Liquid} = -1276 - 5.3873 T + 2699(x_{Cr} - x_{Ni})$$

$$L_{Mo,Ni}^{Liquid} = -46540 + 19.53 T + 2915(x_{Mo} - x_{Ni})$$

### The Bcc Phase

1 sublattice, Constituents Cr,Mo,Ni

298.15 < T < 2180.00

$${}^\circ G_{Cr}^{bcc} - H_{Cr}^{SER} = -8851.93 + 157.48 T - 26.908 T \ln T + 0.0189435 T^2 - 1.47721 \cdot 10^{-6} T^3 + 139250 T^{-1}$$

2180.00 < T < 6000.00

$${}^\circ G_{Cr}^{bcc} - H_{Cr}^{SER} = -34864 + 344.18 T - 50 T \ln T - 2.88526 \cdot 10^{32} T^{-9}$$

298.15 < T < 2896.00

$${}^\circ G_{Mo}^{bcc} - H_{Mo}^{SER} = -7747.247 + 131.9197 T - 23.56414 T \ln T - 0.03443396 T^2 + 5.66283 \cdot 10^{-7} T^3 + 65812 T^{-1} - 1.30927 \cdot 10^{-10} T^4$$

2896.00 < T < 5000.00

$${}^\circ G_{Mo}^{bcc} - H_{Mo}^{SER} = -30724.08 + 283.6116 T - 42.63829 T \ln T - 4.610447 \cdot 10^{33} T^{-9}$$

$${}^\circ G_{Ni}^{bcc} = {}^\circ G_{Ni}^{bcc} + 8715.084 - 3.556 T$$

$$L_{Cr,Mo}^{bcc} = +28890 - 7.962 T + (5974 - 2.428 T)(x_{Cr} - x_{Mo})$$

$$L_{Cr,Ni}^{bcc} = +21310 - 13.6585 T + (25800 - 7.8927 T)(x_{Cr} - x_{Ni})$$

$$L_{Mo,Ni}^{bcc} = 46422$$

**Magnetic contribution:** p is 0.4 for bcc. Negative values of Tc and  $\beta$  should be divided by -1 before inserting them in the equation for  $G_m^{mg}$ .

$$Tc^{bcc} = -311.5 x_{Cr} + 575 x_{Ni} + (2372 + 617(x_{Cr} - x_{Ni})) x_{Cr} x_{Ni}$$

$$\beta^{bcc} = -0.01 x_{Cr} + 0.85 x_{Ni} + 4 x_{Cr} x_{Ni}$$

### The Fcc Phase

1 sublattice, Constituents Cr,Mo,Ni

$${}^{\circ}G_{Cr}^{fcc} = {}^{\circ}G_{Cr}^{fcc} + 7284 + 0.163 T$$

$${}^{\circ}G_{Mo}^{fcc} = {}^{\circ}G_{Mo}^{fcc} + 15200 + 0.63 T$$

$$298.15 < T < 1728.00$$

$${}^{\circ}G_{Ni}^{fcc} - H_{Ni}^{SER} = -5179.159 + 117.854 T - 22.096 T \ln T - 0.0048407 T^2$$

$$1728.00 < T < 3000.00$$

$${}^{\circ}G_{Ni}^{fcc} - H_{Ni}^{SER} = -27840.655 + 279.135 T - 43.1 T \ln T + 1.12754 \cdot 10^{31} T^{-9}$$

$$L_{Cr,Ni}^{fcc} = +8347 - 12.1038 T + (29895 - 16.3838 T)(x_{Cr} - x_{Ni})$$

$$L_{Mo,Ni}^{fcc} = +4803.7 - 5.96 T + 10880(x_{Mo} - x_{Ni})$$

**Magnetic contribution:** p is 0.28 for fcc. Negative values of Tc and  $\beta$  should be divided by -3 before inserting them in the equation for  $G_m^{mg}$ .

$$Tc^{fcc} = -1109 x_{Cr} + 633 x_{Ni} - 3605 x_{Cr} x_{Ni}$$

$$\beta^{fcc} = -2.46 x_{Cr} + 0.52 x_{Ni} - 1.91 x_{Cr} x_{Ni}$$

### The $\delta$ Phase

3 sublattices, sites 24 : 20 : 12, Constituents Cr,Ni : Cr,Mo,Ni : Mo

$$* {}^{\circ}G_{Cr:Cr:Mo}^{\delta} = +24 {}^{\circ}G_{Cr}^{fcc} + 20 {}^{\circ}G_{Cr}^{bcc} + 12 {}^{\circ}G_{Mo}^{bcc} + 50000$$

$$* {}^{\circ}G_{Ni:Cr:Mo}^{\delta} = +24 {}^{\circ}G_{Ni}^{fcc} + 20 {}^{\circ}G_{Cr}^{bcc} + 12 {}^{\circ}G_{Mo}^{bcc} - 200000$$

$$* {}^{\circ}G_{Cr:Mo:Mo}^{\delta} = +24 {}^{\circ}G_{Cr}^{fcc} + 20 {}^{\circ}G_{Mo}^{bcc} + 12 {}^{\circ}G_{Mo}^{bcc} + 100000$$

$${}^{\circ}G_{Ni:Mo:Mo}^{\delta} = +24 {}^{\circ}G_{Ni}^{fcc} + 32 {}^{\circ}G_{Mo}^{bcc} - 212100 + 1089 T - 142 T \ln T$$

$$* {}^{\circ}G_{Cr:Ni:Mo}^{\delta} = +24 {}^{\circ}G_{Cr}^{fcc} + 20 {}^{\circ}G_{Ni}^{bcc} + 12 {}^{\circ}G_{Mo}^{bcc} - 200000$$

$${}^{\circ}G_{Ni:Ni:Mo}^{\delta} = +24 {}^{\circ}G_{Ni}^{fcc} + 20 {}^{\circ}G_{Ni}^{bcc} + 12 {}^{\circ}G_{Mo}^{bcc} - 1030 - 93.5 T + 13.5 T \ln T$$

### The P Phase

3 sublattices, sites 24 : 20 : 12, Constituents Cr,Ni : Cr,Mo,Ni : Mo

$$* \circ G_{Cr:Cr:Mo}^P = +24 \circ G_{Cr}^{fcc} + 20 \circ G_{Cr}^{bcc} + 12 \circ G_{Mo}^{bcc} + 252300 - 100 T$$

$$* \circ G_{Ni:Cr:Mo}^P = +24 \circ G_{Ni}^{fcc} + 20 \circ G_{Cr}^{bcc} + 12 \circ G_{Mo}^{bcc} - 341858$$

$$* \circ G_{Cr:Mo:Mo}^P = +24 \circ G_{Cr}^{fcc} + 20 \circ G_{Mo}^{bcc} + 12 \circ G_{Mo}^{bcc} + 95573 - 200 T$$

$$\circ G_{Ni:Mo:Mo}^P = +24 \circ G_{Ni}^{fcc} + 20 \circ G_{Mo}^{bcc} + 12 \circ G_{Mo}^{bcc} + 26739 - 100 T$$

$$* \circ G_{Cr:Ni:Mo}^P = +24 \circ G_{Cr}^{fcc} + 20 \circ G_{Ni}^{bcc} + 12 \circ G_{Mo}^{bcc} - 434085$$

$$\circ G_{Ni:Ni:Mo}^P = +24 \circ G_{Ni}^{fcc} + 20 \circ G_{Ni}^{bcc} + 12 \circ G_{Mo}^{bcc} + 205845 - 100 T$$

### The $\sigma$ Phase

3 sublattices, sites 8 : 4 : 18, Constituents Ni : Cr,Mo : Cr,Mo,Ni

$$\circ G_{Ni:Cr:Cr}^{\sigma} = +8 \circ G_{Ni}^{fcc} + 22 \circ G_{Cr}^{bcc} + 173460 - 188 T$$

$$* \circ G_{Ni:Mo:Cr}^{\sigma} = +8 \circ G_{Ni}^{fcc} + 4 \circ G_{Mo}^{bcc} + 18 \circ G_{Cr}^{bcc} + 386423$$

$$* \circ G_{Ni:Cr:Mo}^{\sigma} = +8 \circ G_{Ni}^{fcc} + 4 \circ G_{Cr}^{bcc} + 18 \circ G_{Mo}^{bcc} - 131651$$

$$* \circ G_{Ni:Mo:Mo}^{\sigma} = +8 \circ G_{Ni}^{fcc} + 22 \circ G_{Mo}^{bcc} + 85662$$

$$\circ G_{Ni:Cr:Ni}^{\sigma} = +8 \circ G_{Ni}^{fcc} + 4 \circ G_{Cr}^{bcc} + 18 \circ G_{Ni}^{bcc} + 175400$$

$$* \circ G_{Ni:Mo:Ni}^{\sigma} = +8 \circ G_{Ni}^{fcc} + 4 \circ G_{Mo}^{bcc} + 18 \circ G_{Ni}^{bcc} - 16385$$

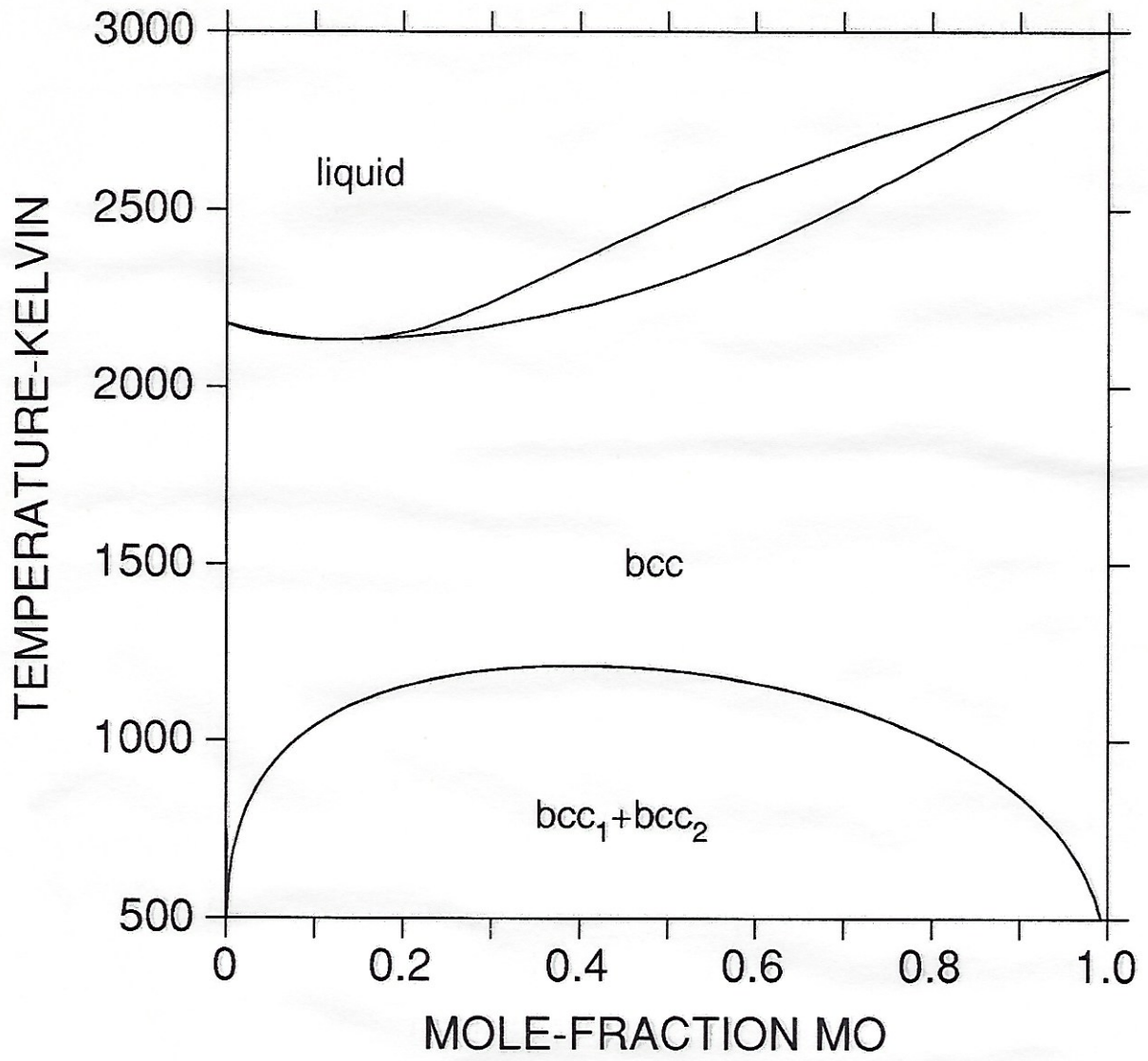


Fig.1. The calculated Cr-Mo phase diagram according to Ref.3.

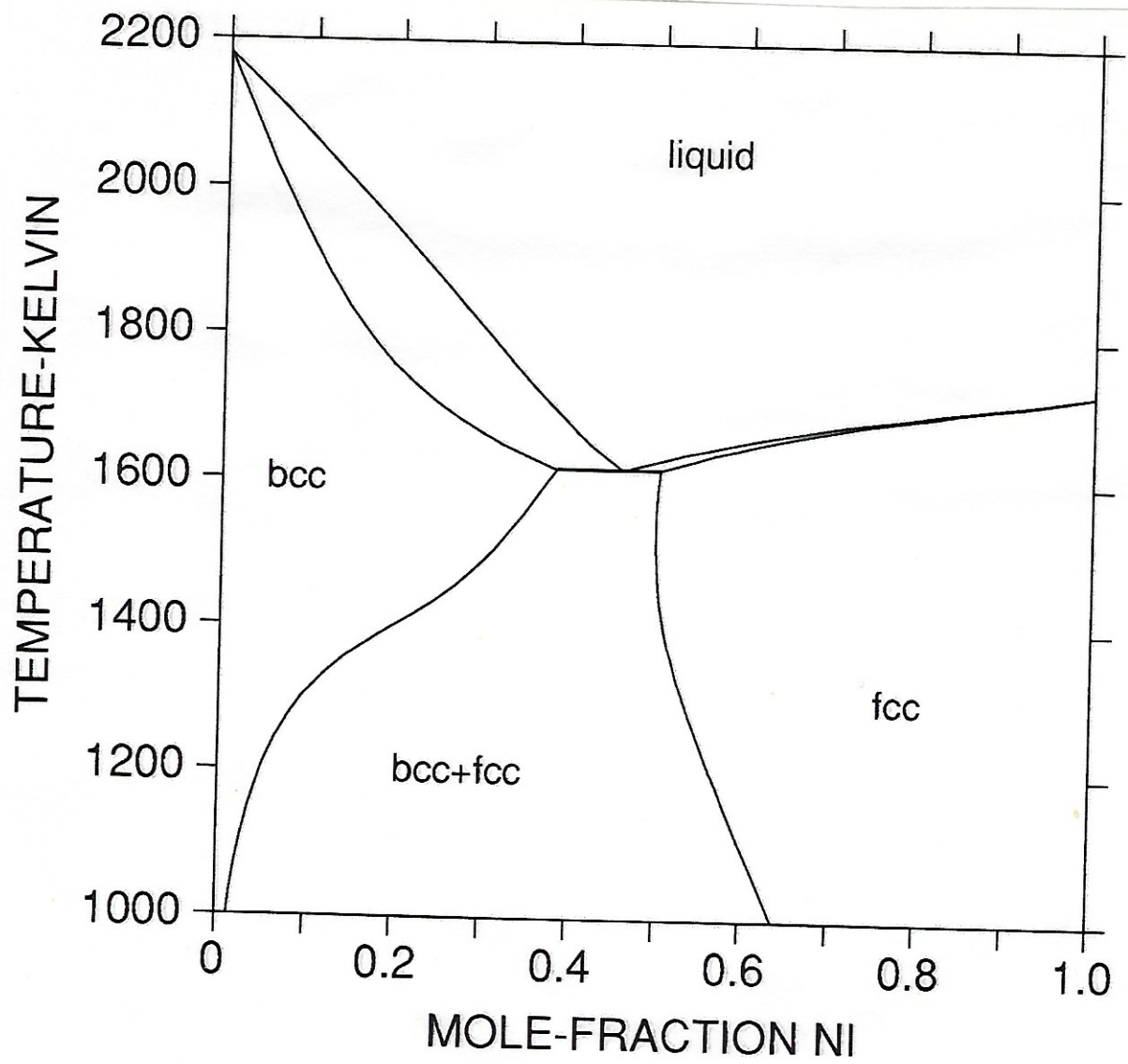


Fig.2. The calculated Cr-Ni phase diagram according to Ref.4.

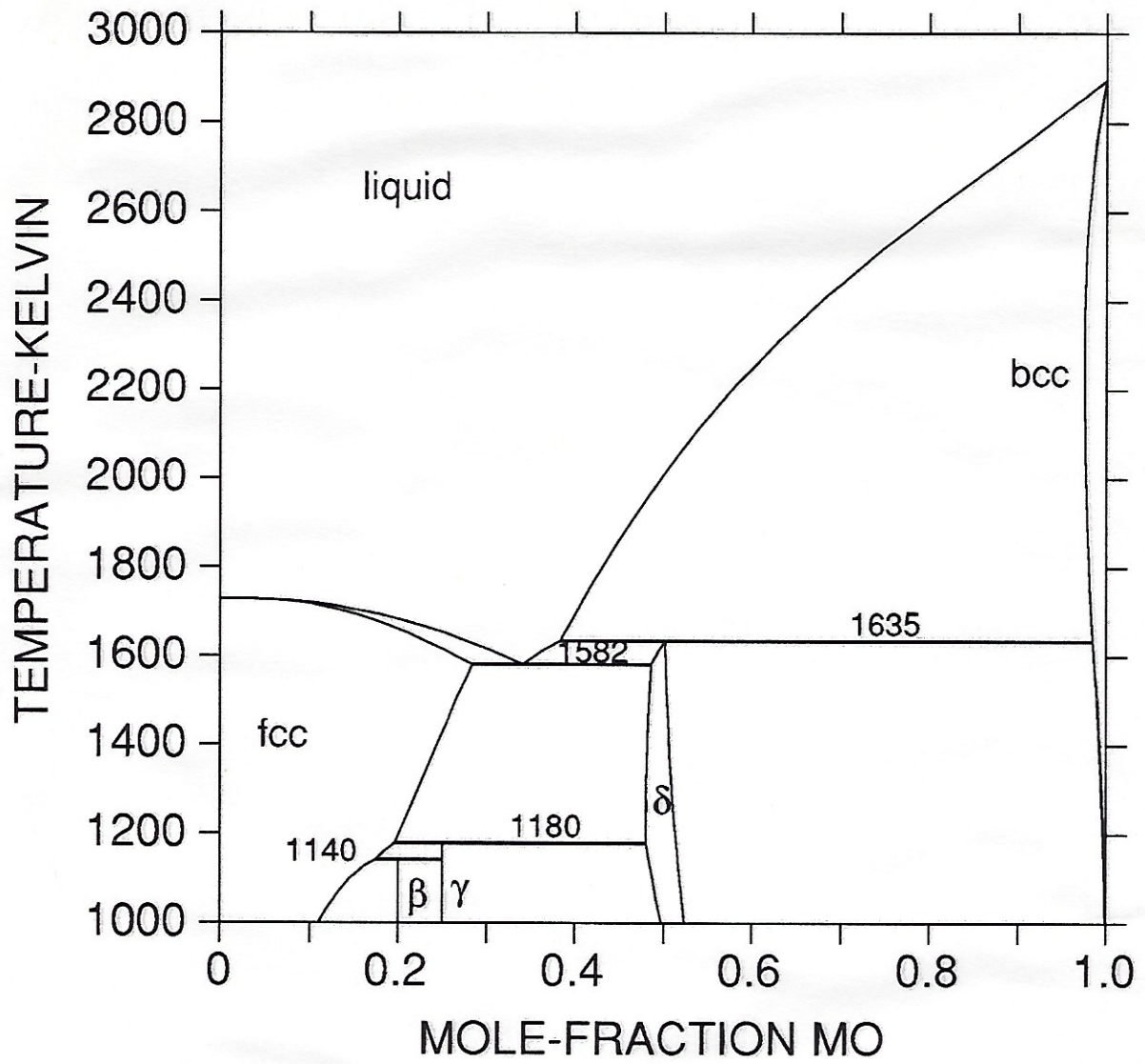


Fig.3. The calculated Mo-Ni phase diagram according to Ref.5.

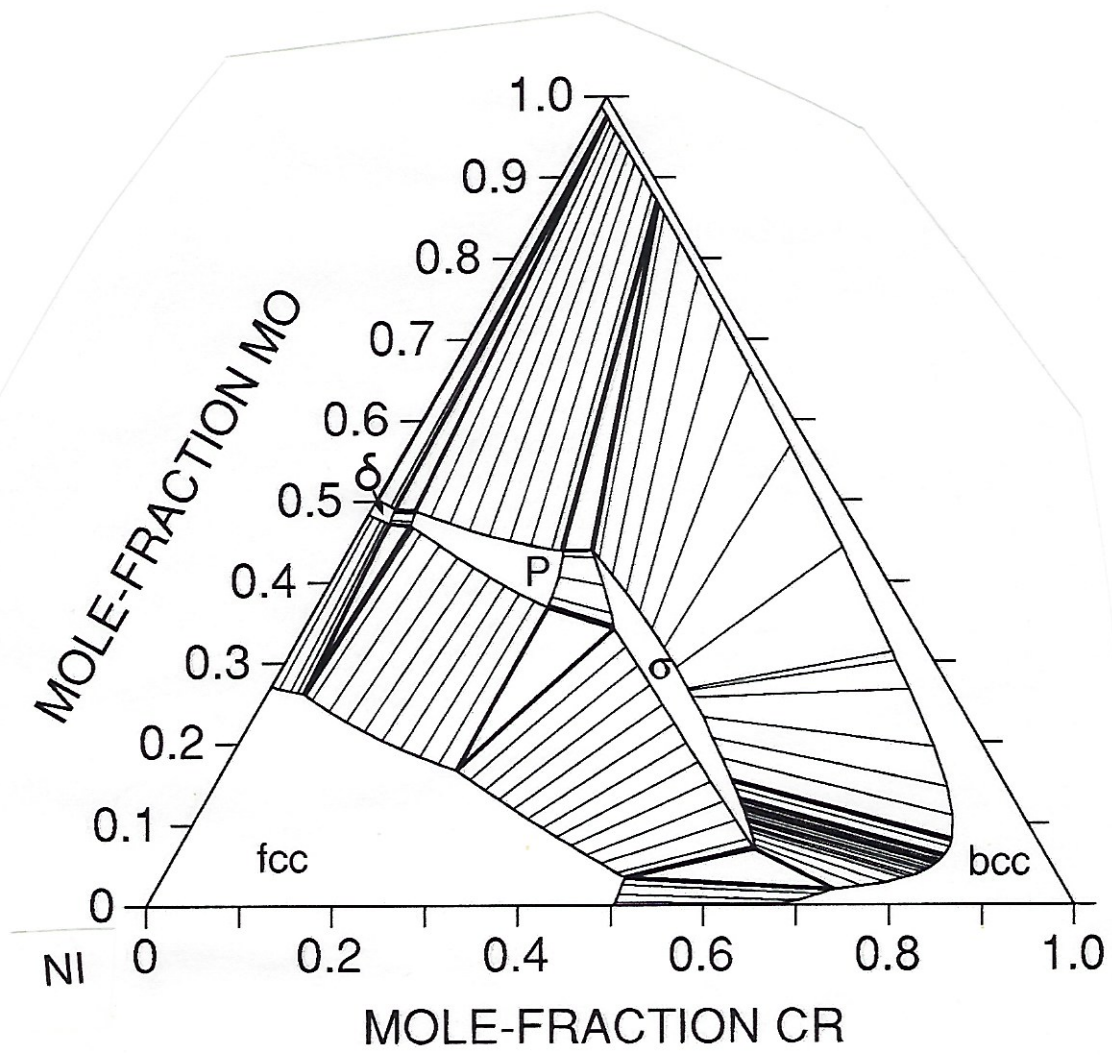


Fig.4. The calculated isothermal section at 1523K.

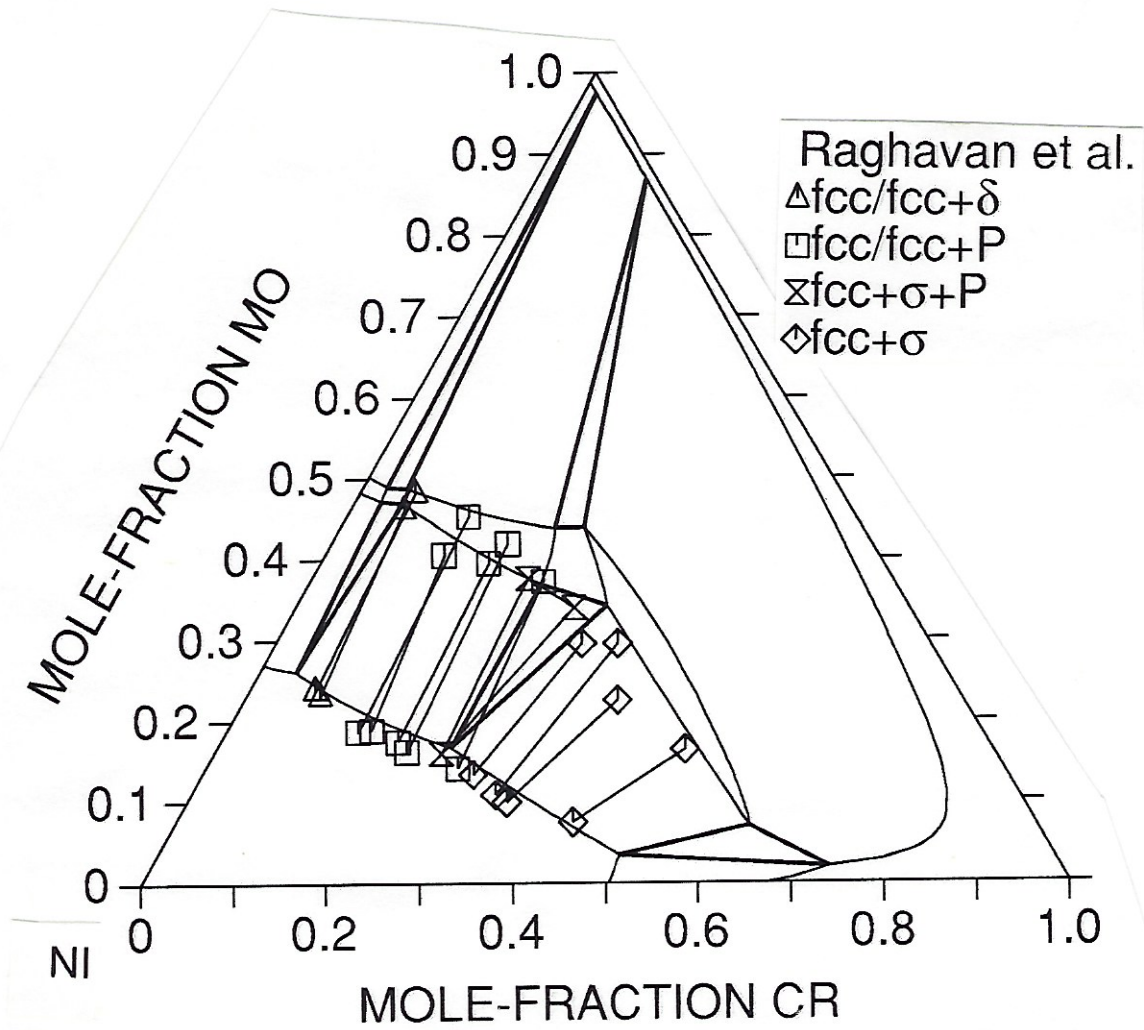


Fig.5. The calculated isothermal section at 1523K together with experimental data by Raghavan et al.<sup>8</sup>.

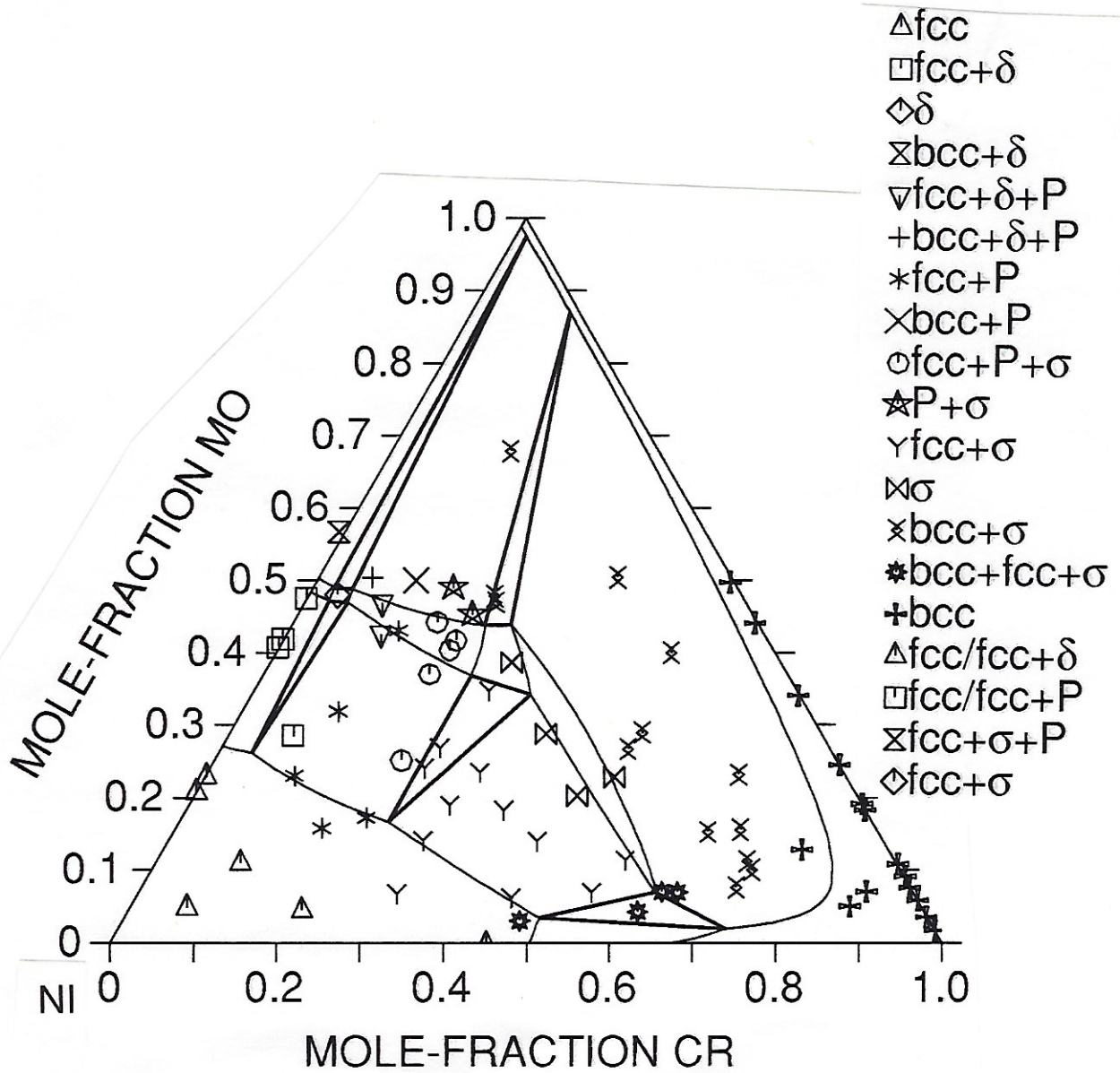


Fig.6. The calculated isothermal section at 1523K together with experimental data by Bloom and Grant<sup>7</sup>.

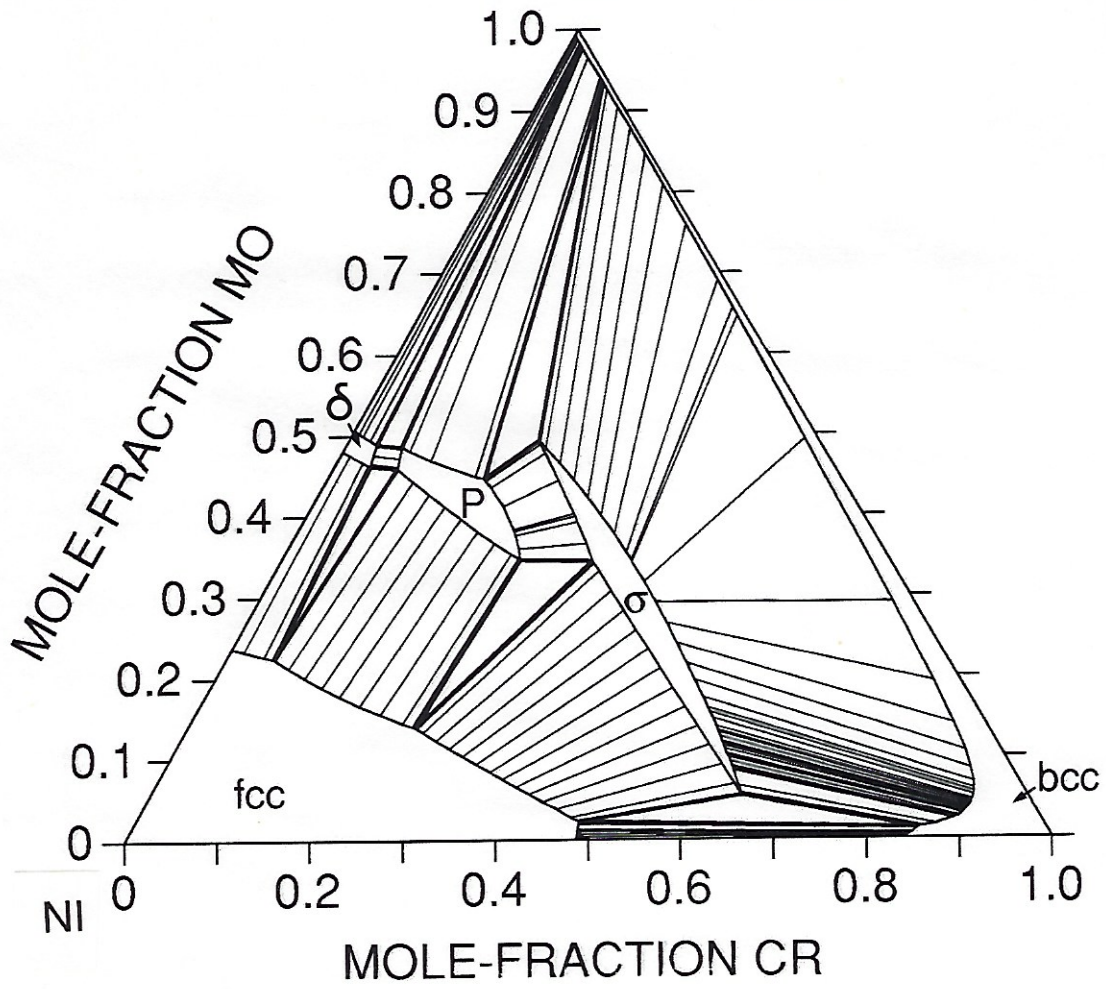


Fig.7. The calculated isothermal section at 1373K.

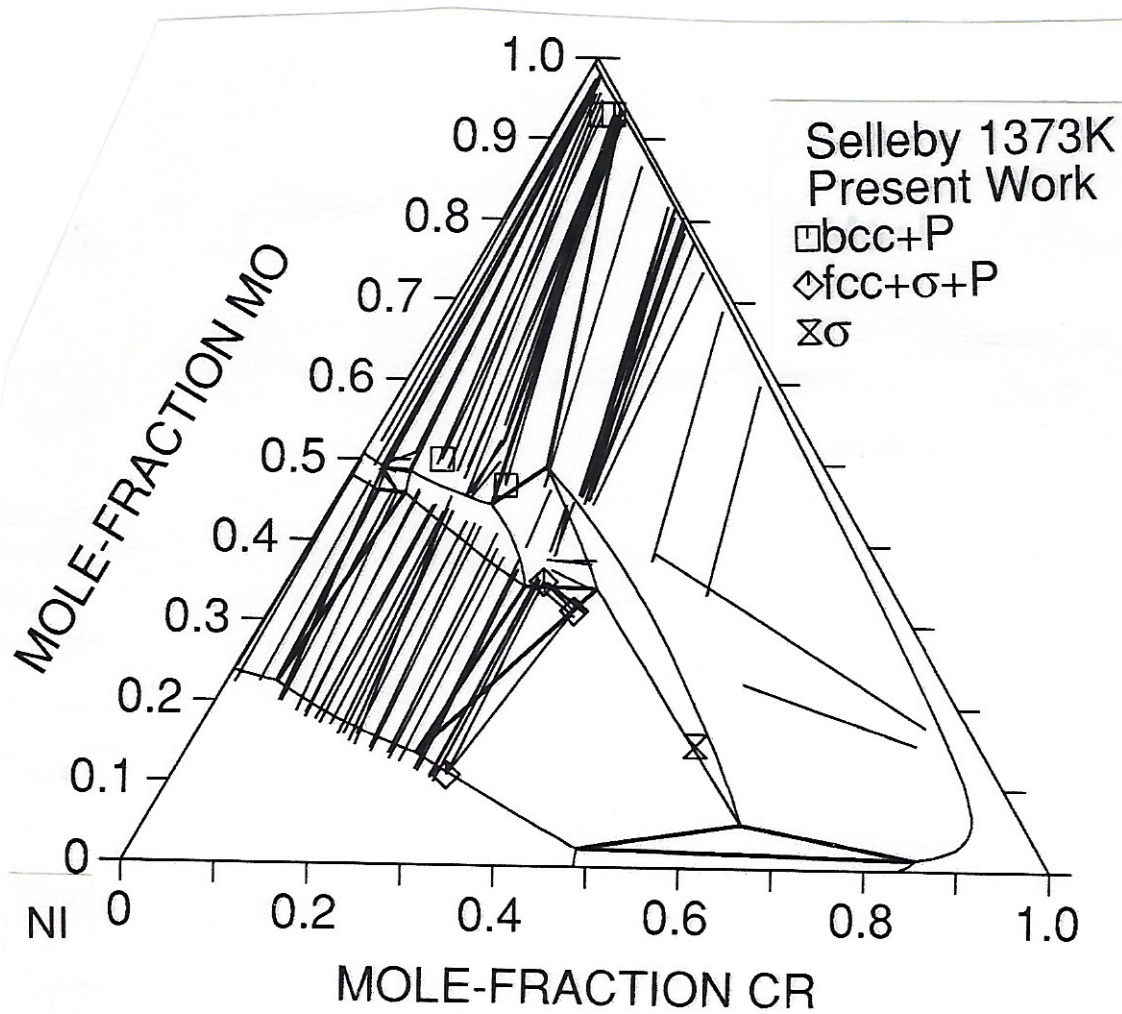


Fig.8. The calculated isothermal section at 1373K together with experimental data by Selleby<sup>2</sup>, and experimental results from the present work. The tielines measured in the present work are marked with symbols. The phases in the samples marked "bcc+P" and "σ" were identified by X-ray diffraction in the present work.

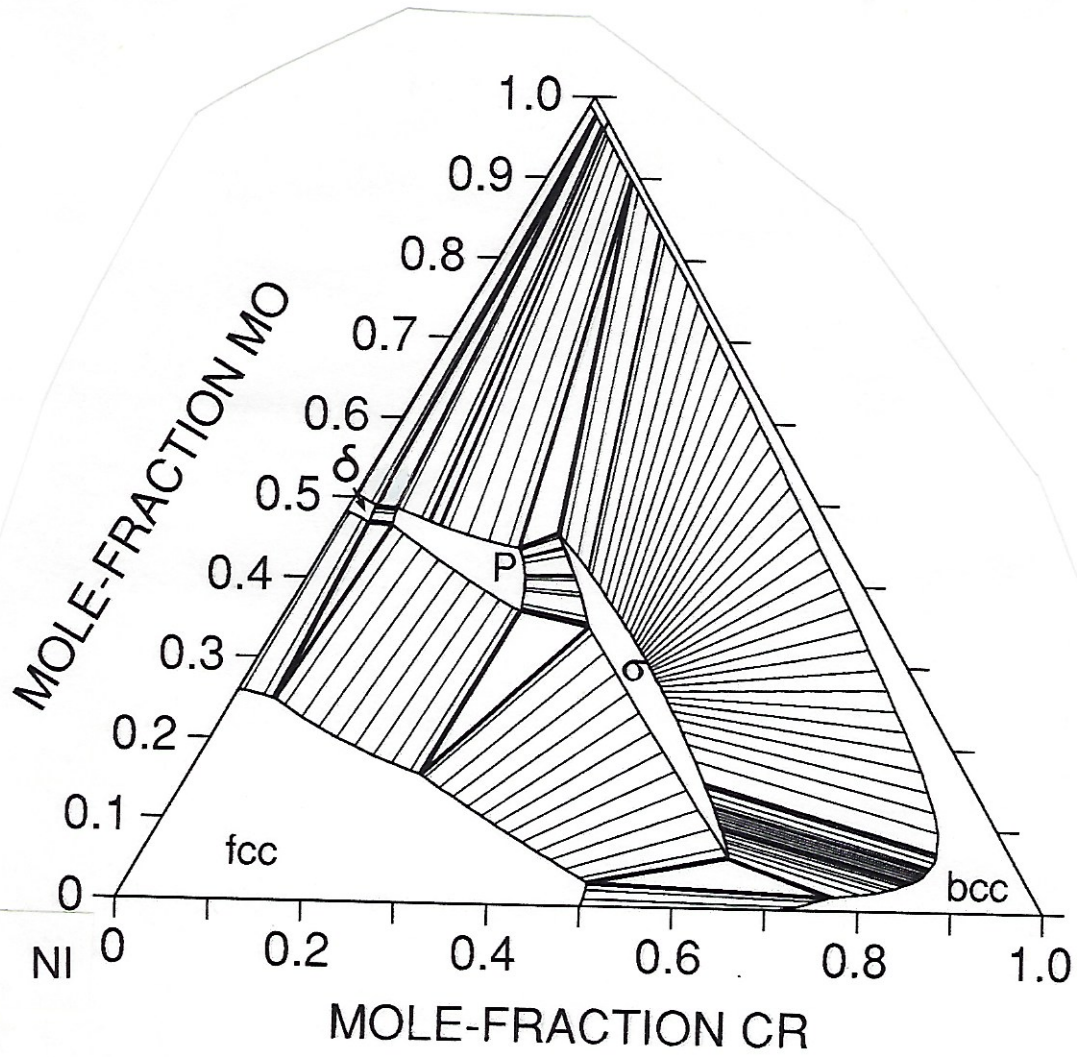


Fig.9. The calculated isothermal section at 1473K.

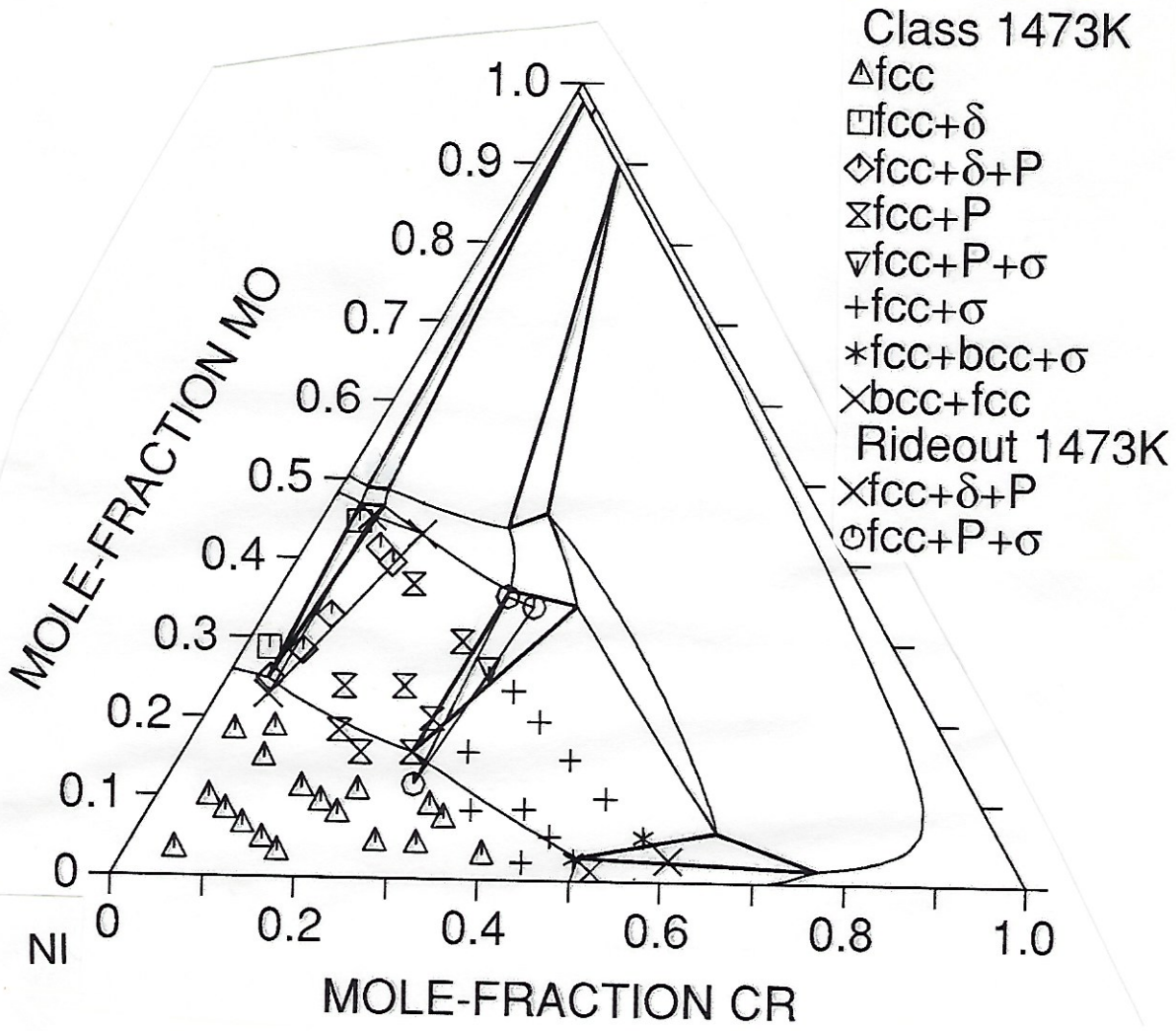


Fig.10. The calculated isothermal section at 1473K, together with experimental data from the studies by Class et al.<sup>9</sup>, and by Rideout et al.<sup>6</sup>.

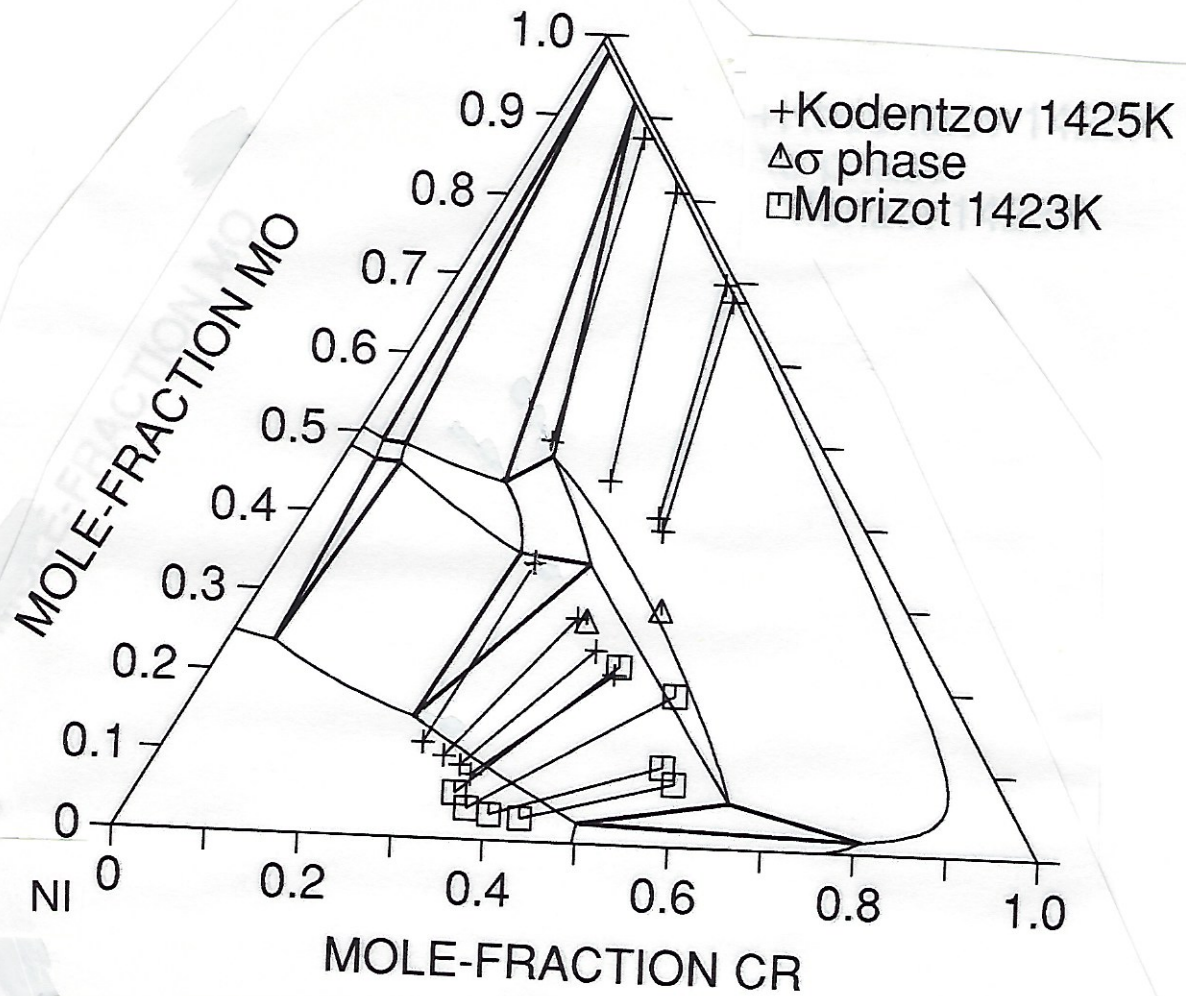


Fig.11. The calculated isothermal section at 1425K compared with experimental data by Morizot and Vignes<sup>10</sup>, and Kodentzov et al.<sup>11</sup>.

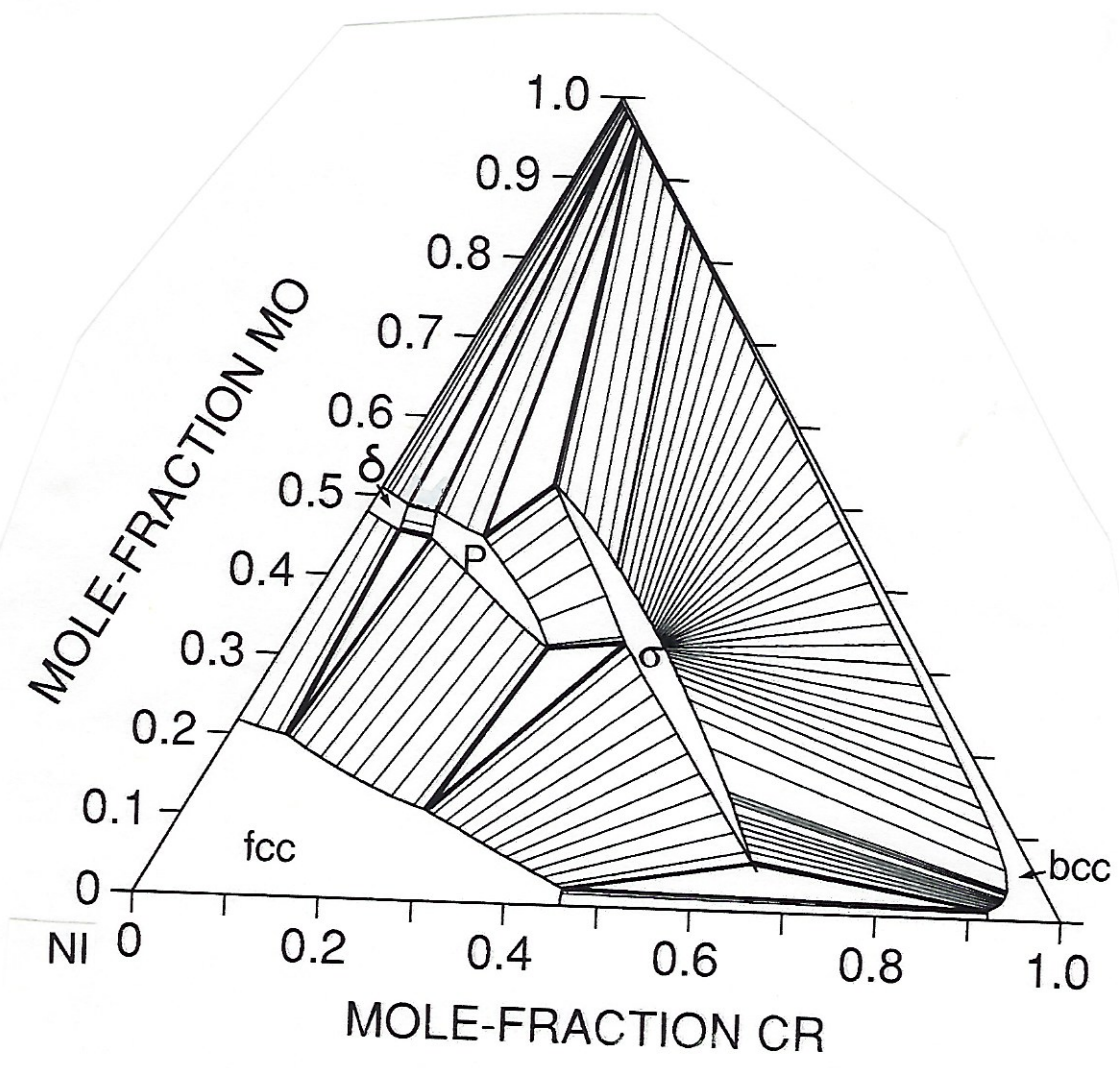


Fig.12. The calculated isothermal section at 1273K.

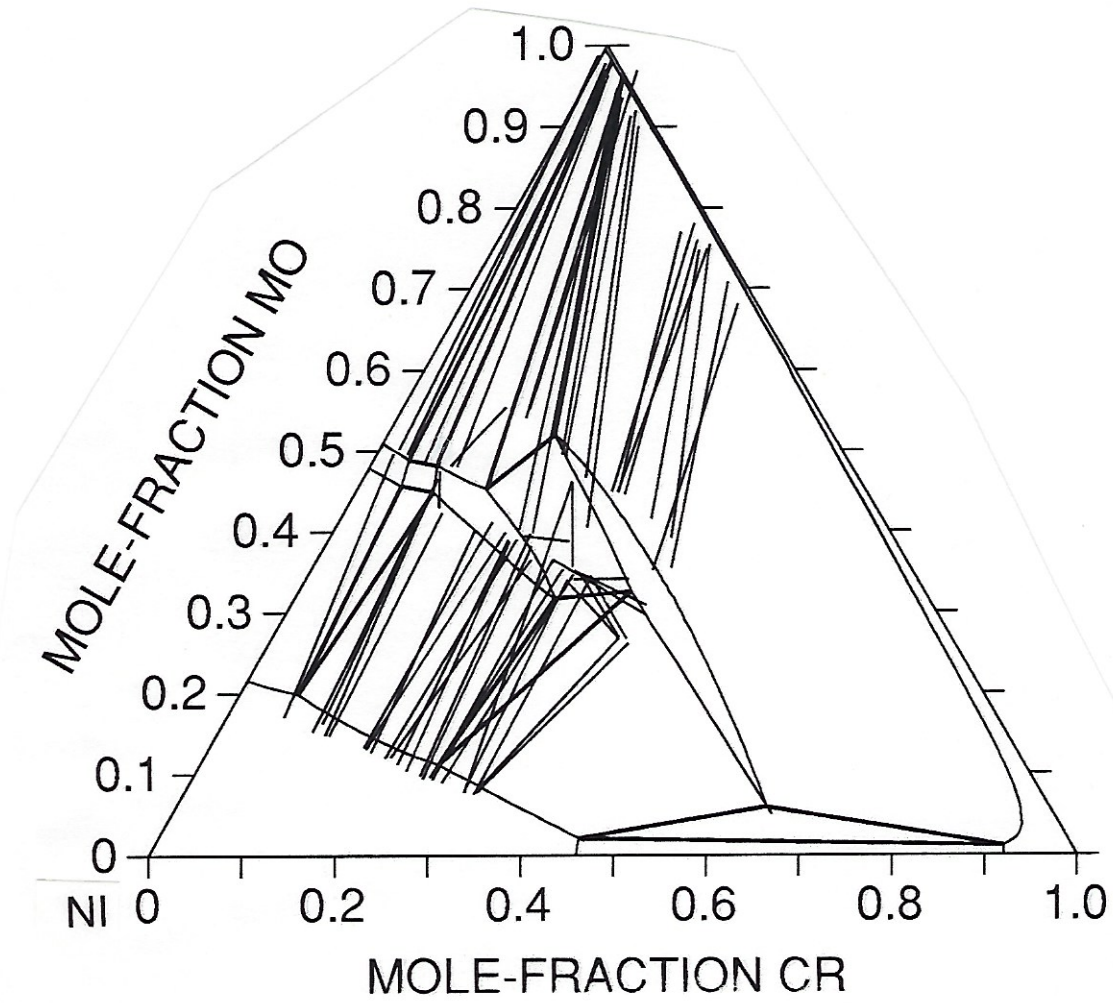


Fig.13. The calculated isothermal section at 1273K compared with experimental data from Ref.2.

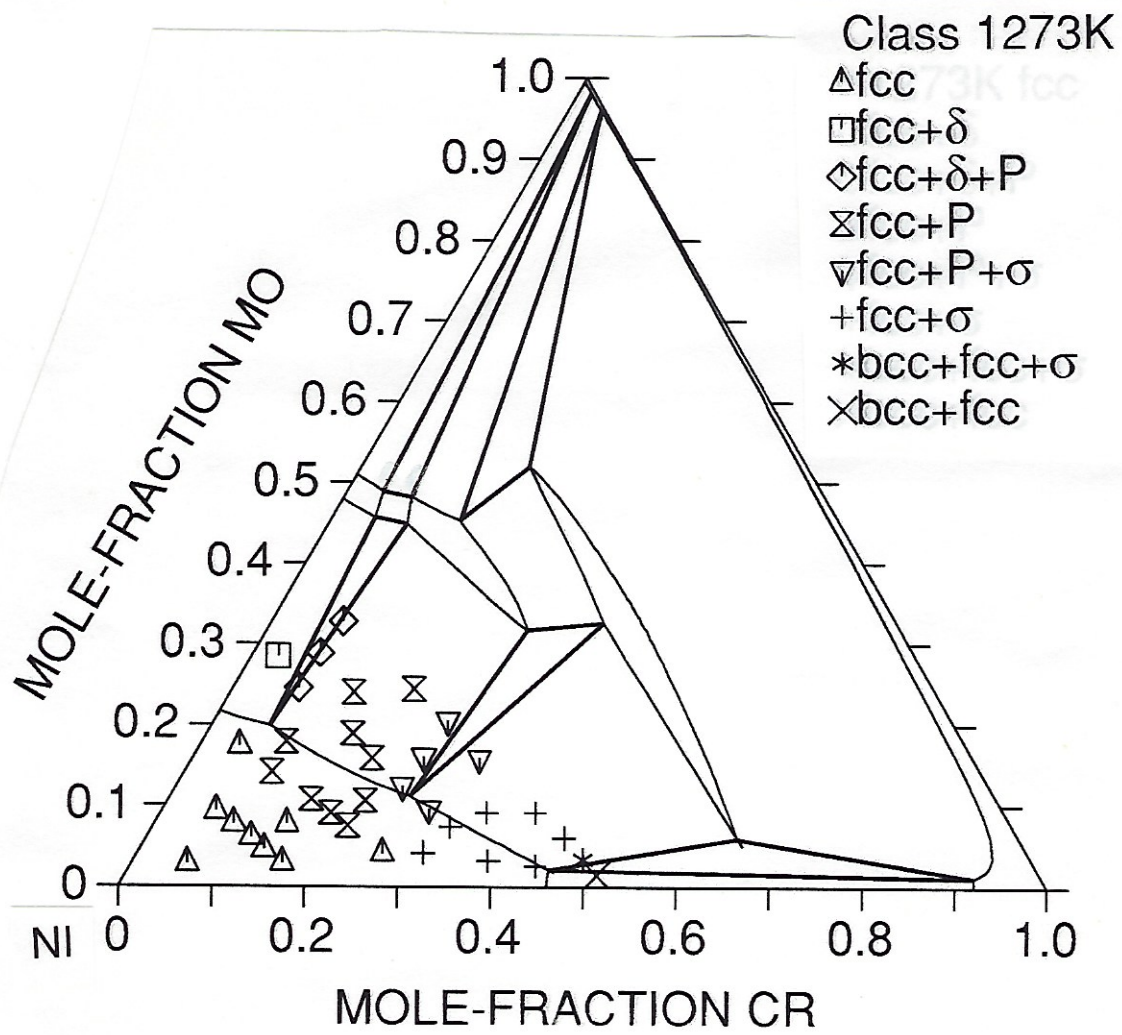


Fig.14. The calculated isothermal section at 1273K compared with experimental data by Class et al.<sup>9</sup>.

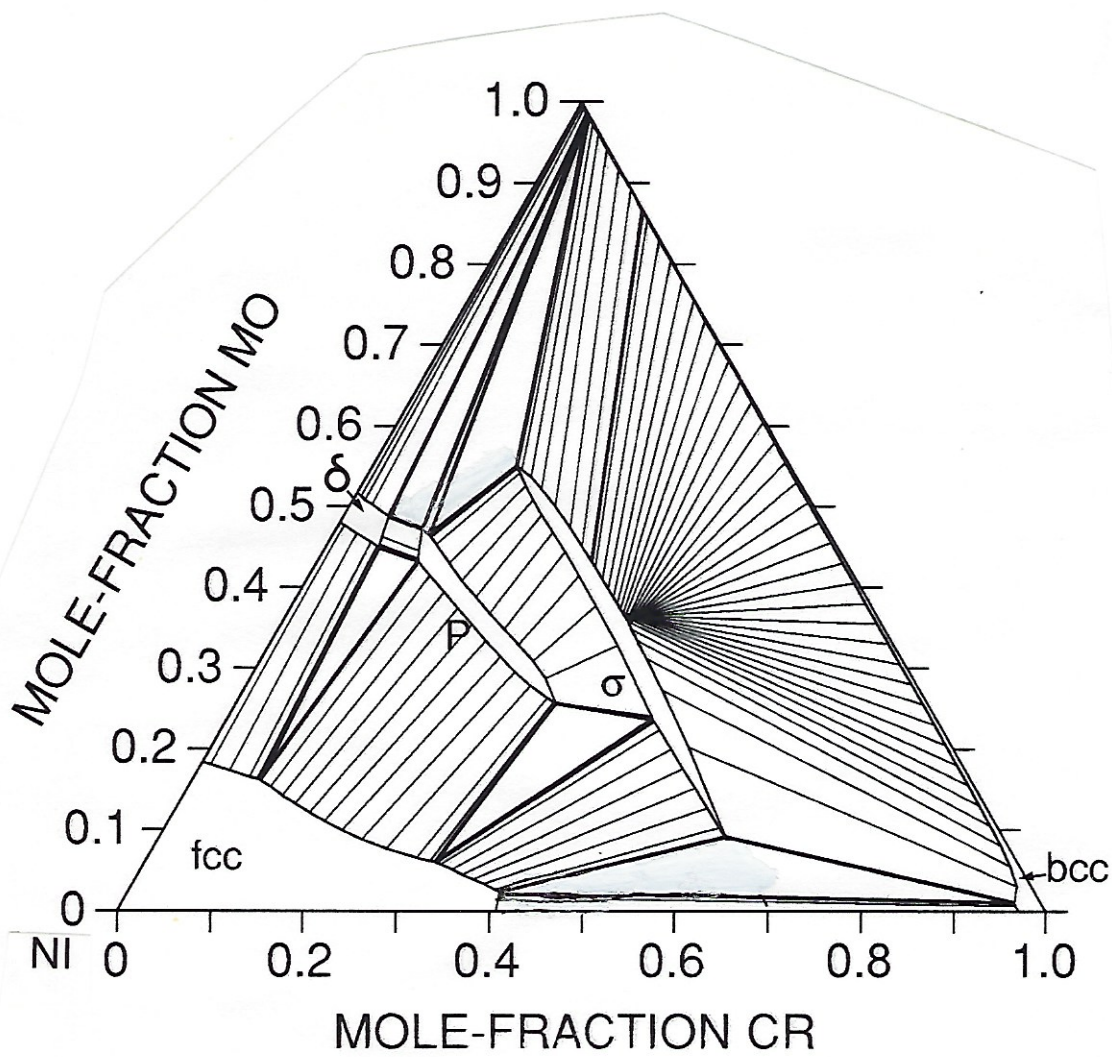


Fig.15. The calculated isothermal section at 1123K, excluding the  $\mu$ ,  $\beta$  and  $\gamma$  phases.

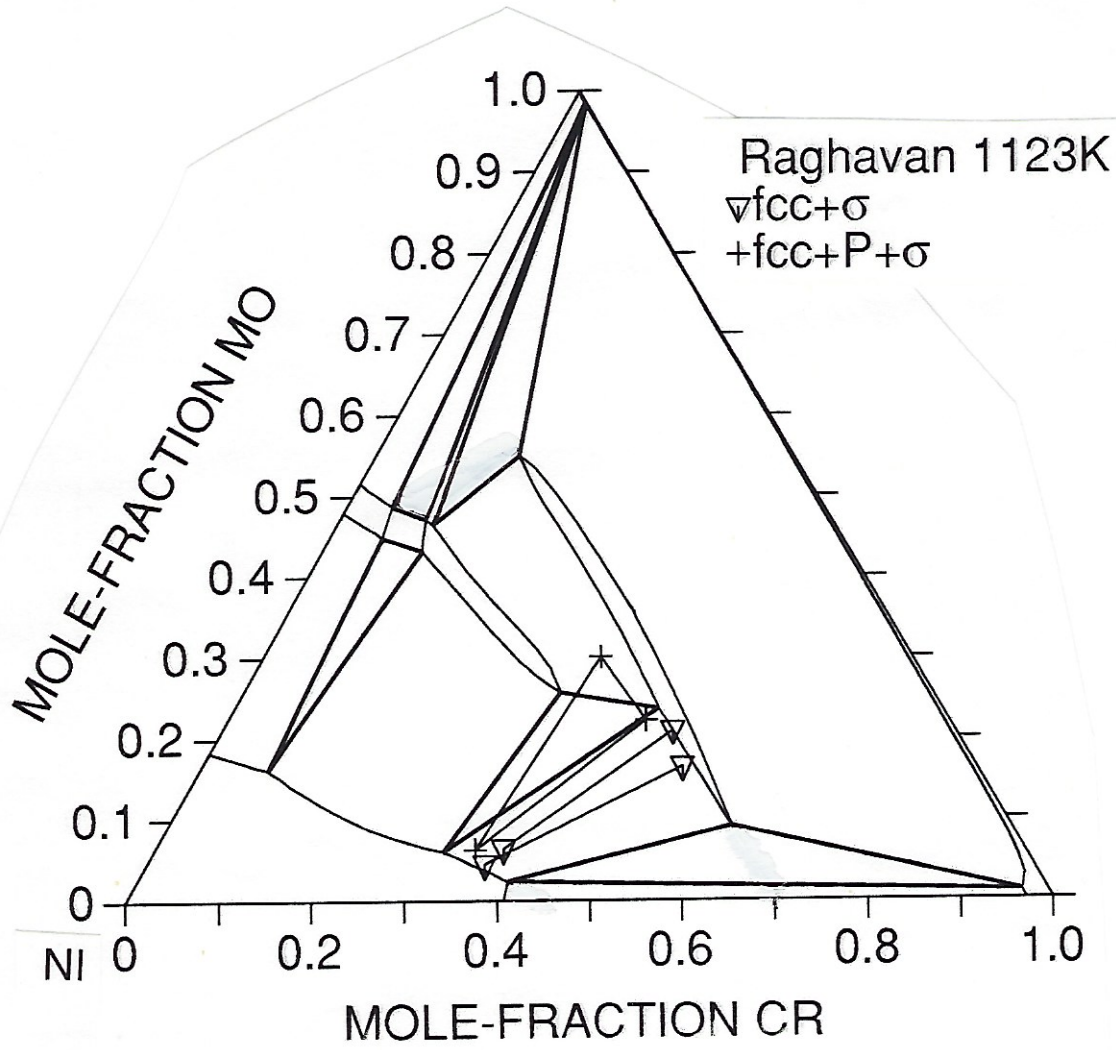


Fig.16. The calculated isothermal section at 1123K together with experimental data by Raghavan et al.<sup>8</sup>

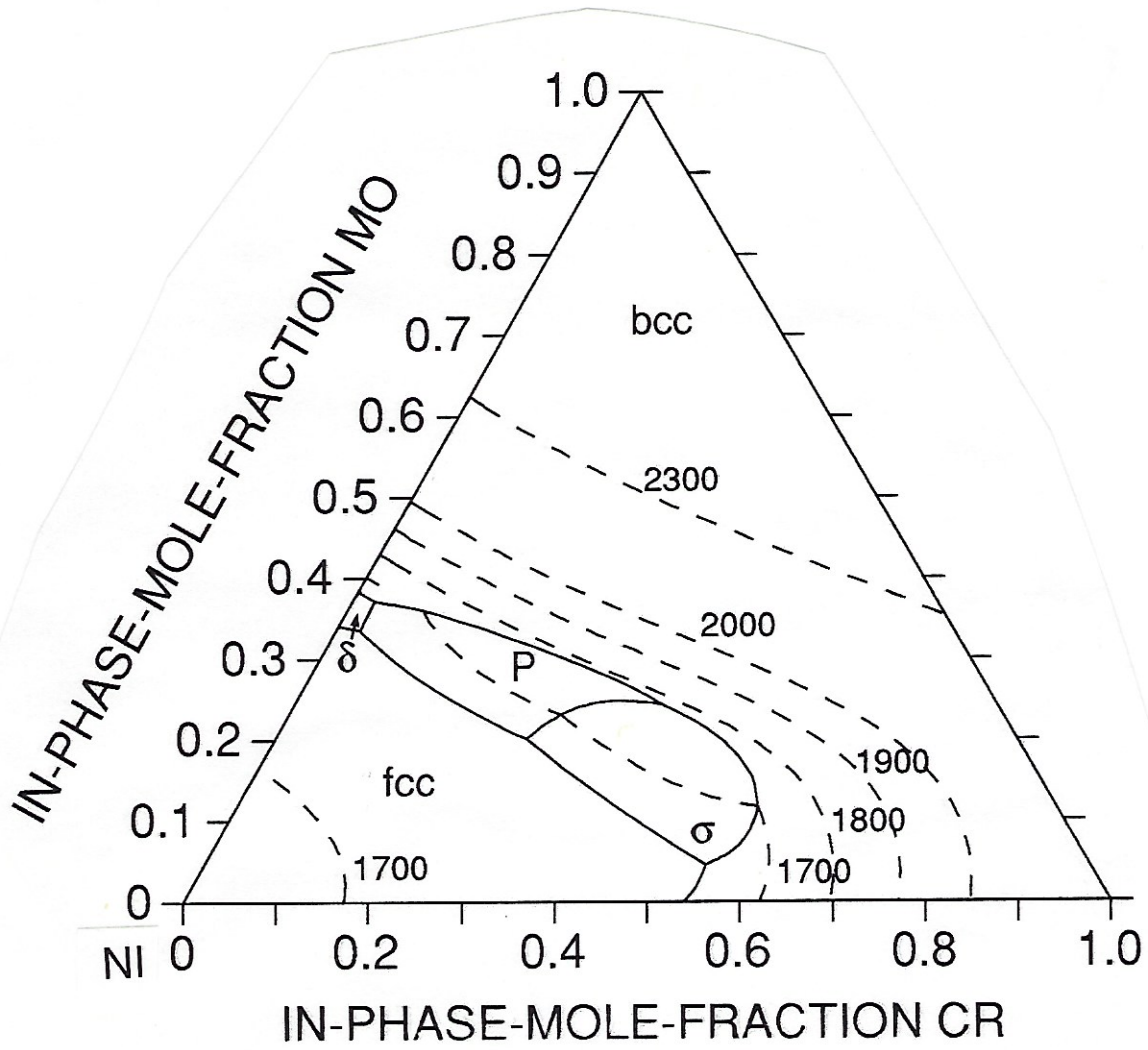


Fig.17. The calculated projection of the liquidus surface. The dashed lines represent isotherms at 1700, 1800, 1900, 2000 and 2300K.

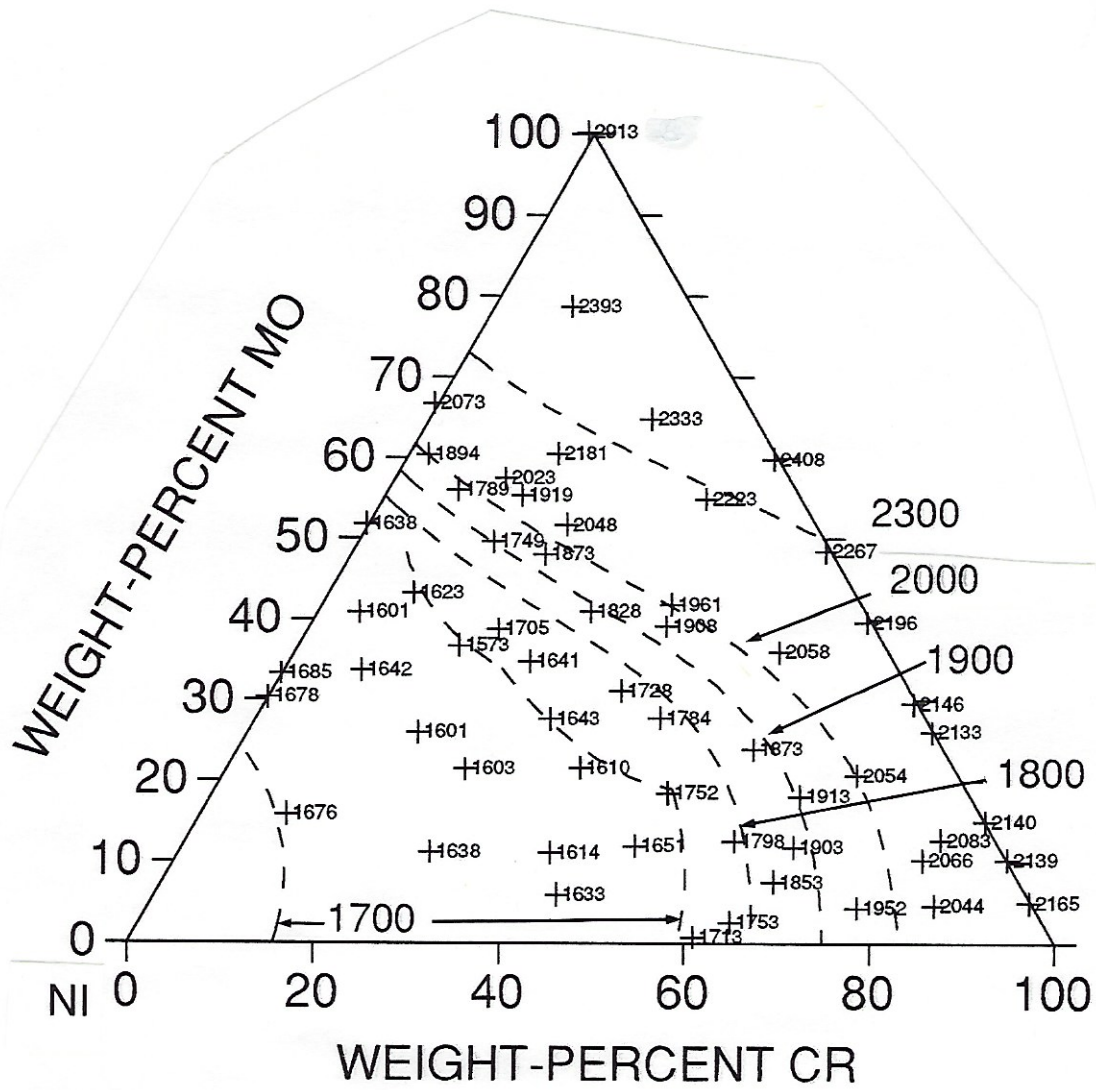


Fig.18. The calculated isotherms from Fig.17 together with the experimental information on liquidus temperatures by Bloom and Grant<sup>7</sup>.